

Persistent spin helix on a wurtzite ZnO(10⁻¹⁰) surface: First-principles density-functional study

メタデータ	言語: eng 出版者: 公開日: 2017-10-03 キーワード (Ja): キーワード (En): 作成者: メールアドレス: 所属:
URL	https://doi.org/10.24517/00010736

This work is licensed under a Creative Commons Attribution-NonCommercial-ShareAlike 3.0 International License.



Persistent spin helix on a wurtzite ZnO ($10\bar{1}0$) surface: First-principles density-functional study

Moh Adhib Ulil ABSOR^{1,2}, Fumiyuki ISHII³, Hiroki KOTAKA¹, and Mineo SAITO³

¹*Graduate School of Natural Science and Technology, Kanazawa University, Kanazawa 920-1192, Japan*

²*Department of Physics Universitas Gadjah Mada BLS 21 Yogyakarta Indonesia*

³*Faculty of Mathematics and Physics, Institute of Science and Engineering, Kanazawa University, Kanazawa 920-1192, Japan*

The persistent spin helix (PSH) that has been widely and exclusively studied in zinc-blende structures is revealed for the first time on the surface of a wurtzite structure. Through first-principles calculations of the ZnO ($10\bar{1}0$) surface, a quasi-one dimensional orientation of the spin textures is identified. Further, the wavelength of this particular PSH is smaller than that observed with various zinc-blende quantum well structures, thus indicating that wurtzite-structured surfaces are suitable for spintronics applications.

Spin-orbit coupled systems have attracted considerable scientific interest over recent years, as they allow for the manipulation of electron spin.¹⁾ This spin-orbit coupling (SOC) plays an important role in new fundamental phenomena such as current-induced spin polarization²⁾ and the spin Hall effect.³⁾ The electric tunability of SOC has also been achieved by using gated semiconductor heterostructures,⁴⁾ thereby opening a new gateway to applications ranging from spintronics to quantum computing. Examples of some of the various spintronics devices that have already been studied include spin-field effect transistors,⁵⁾ spin filters,⁶⁾ and spin qubit gates.⁷⁾

Energy-saving spintronics devices are believed to be possible using persistent spin helix (PSH) materials, as these induce a greatly enhanced spin relaxation time.⁸⁻¹⁵⁾ Theoretical studies have predicted that such PSH materials can be produced using [001]-oriented quantum wells (QWs) in which the Rashba and Dresselhaus terms are equal, or by using [110]-oriented QWs that are only affected by the Dresselhaus effect.⁸⁾ In either case, the spin-orbit coupling is linearly dependent on the electron momentum in specific directions, and so a one-dimensional orientation of the spin textures is generated.⁸⁾ The PSH states have been observed experimentally for [001]-oriented GaAs/AlGaAs QWs^{9,10,14)} and InAlAs/InGaAs QWs,¹¹⁻¹³⁾ as well as for [110]-oriented GaAs/AlGaAs QWs that exhibit uni-directional out-of-plane spin directions.¹⁵⁾

Up till now, PSH has only been widely studied with zinc-blende semiconductors. However, experimental observation of high-quality two-dimensional systems in wurtzite-structured

semiconductors^{16,17)} has seen them become increasingly viewed as a promising candidate for spintronics applications.¹⁸⁾ As such, there is clearly great value in achieving PSH in these semiconductors. In this Letter, we demonstrate that PSH is possible using a wurtzite ZnO (10 $\bar{1}$ 0) surface. By performing first-principles density functional theory (DFT) calculations of the ZnO (10 $\bar{1}$ 0) surface, a quasi-one-dimensional orientation of the spin textures is identified and clarified by using a simplified spin-orbit Hamiltonian. Finally, it is revealed that the wavelength of this PSH is smaller than that seen with various zinc-blende QW structures.

First-principles electronic-structure calculations based on the DFT were carried out within a generalized gradient approximation (GGA)¹⁹⁾ using the OpenMX code.²⁰⁾ In a previous study, it was found that the optimized lattice parameters of bulk ZnO are $a = 3.284 \text{ \AA}$ and $c/a = 1.615$.¹⁸⁾ Surface calculations were carried out using a slab model consisting of 20-bilayers and terminated by hydrogen atoms on its backside [Fig. 1(a)]. The vacuum length was set to more than 15 \AA in order to avoid interactions between neighboring slabs. Geometries were fully relaxed until the force acting on each atom was less than 1 meV/ \AA . Norm-conserving pseudo-potentials²¹⁾ were used. The wave functions were expanded by a linear combination of multiple pseudo-atomic orbitals (LCPAOs) generated using a confinement scheme,^{22,23)} being defined as Zn6.0- $s^2p^2d^2$, O5.0- $s^2p^2d^1$, and H5.0- s^2p^1 . For example, in the case of a Zn atom, Zn6.0- $s^2p^2d^2$ means that in this confinement scheme the cutoff radius is 6.0 Bohr^{22,23)} and two primitive orbitals for the s , p , and d components are used. SOC was included in these fully-relativistic calculations, and the spin textures in k -space were calculated using the k -space spin density matrix of the spinor wave function.²⁴⁾

Calculations for a ZnO (10 $\bar{1}$ 0) surface identified that the out-of-plane relaxation of Zn and O atoms are $\delta_z(\text{Zn}) = -0.28 \text{ \AA}$ and $\delta_z(\text{O}) = -0.035 \text{ \AA}$, respectively [Fig. 1(a)]. These values are slightly smaller than previous experimental values of $\delta_z(\text{Zn}) = -0.45 \text{ \AA}$ and $\delta_z(\text{O}) = -0.05 \text{ \AA}$,²⁵⁾ but are in a good agreement with past calculations [-0.36 to -0.21 \AA ($\delta_z(\text{Zn})$) and -0.04 \AA ($\delta_z(\text{O})$)].²⁶⁻²⁸⁾ On the other hand, the in-plane relaxations of Zn and O atoms, $\delta_y(\text{Zn}) = 0.19 \text{ \AA}$ and $\delta_y(\text{O}) = -0.03 \text{ \AA}$, respectively, are close to prior calculations [$\delta_y(\text{Zn}) = 0.116 \text{ \AA}$ and $\delta_y(\text{O}) = -0.024 \text{ \AA}$].²⁸⁾ Occupied surface states were seen to appear in band structures in the energy range of -1.3 to -0.65 eV [Fig. 1(b),(c)], from which the partial density of states (PDOS) was calculated through projection onto the surface atoms [Fig. 1(d)]. This found that the occupied surface state is characterized by O-2 p orbitals, which is consistent with the results of past calculations using a local density approximation (LDA).²⁷⁾

Given that the surface states are occupied, doping is expected to create a p-type system. Indeed, several studies have succeeded in producing p-type, non-polar wurtzite ZnO films,^{29,30)} giving credence to the notion of creating a p-type wurtzite ZnO (10 $\bar{1}$ 0) surface.

The effect of SOC on the surface states can be seen in Fig. 2, wherein the band splitting is small in the $\bar{\Gamma}$ - \bar{Y} direction, but quite large in the $\bar{\Gamma}$ - \bar{X} direction. In these spin-split surface state

bands, we find that the spin textures exhibit a quasi-one-dimensional orientation in the in-plane y direction [Fig. 3(a)], yet also have out-of-plane z components [Fig. 3(b)]. These quasi-one-dimensional spin textures are expected to generate current in a direction perpendicular to the spin orientation, as well as induce a greatly enhanced spin relaxation time through the PSH mechanism.⁸⁾ This is supported by the fact that a similar PSH has been observed in [110]-oriented zinc-blende QWs with out-of-plane spin orientations.¹⁵⁾

To better understand the origin of spin textures, we must consider the SOC of surface states based on group theory.³¹⁻³⁴⁾ This states that the ZnO (10 $\bar{1}$ 0) surface belongs to the symmetry point group C_s : the mirror reflections in operation in this symmetry transforms (x, y, z) to $(-x, y, z)$. Considering the fact that Hamiltonian SOC is completely symmetric in the C_s point group, and includes first-order terms over the wave vectors, SOC can be expressed as, $H_{SOC} = \alpha_1 k_x \sigma_z + \alpha_2 k_x \sigma_y + \alpha_3 k_y \sigma_x$, where k_x and k_y are the wave vectors in the x and y directions, respectively; σ_x , σ_y , and σ_z are Pauli matrixes; and α_1 , α_2 , and α_3 are coupling constants that define the spin-orbit strength. Here, α_1 is characterized by the in-plane electric field E_y , whereas α_2 and α_3 relate to the out-of-plane electric field E_z that originates from the surface effect.

In the case of a bulk system oriented in the [10 $\bar{1}$ 0] direction, the out-of-plane electric field E_z vanishes. Consequently, in the $k_x - k_y$ plane, both α_2 and α_3 are zero. This leads to a case in which only the first term in the H_{SOC} equation remains, meaning that the bands are spin degenerated in the Γ - Y direction and the spin textures are oriented to the out-of-plane z direction.³⁵⁾ In surface states, on the other hand, a band split is introduced in the $\bar{\Gamma}$ - \bar{Y} direction due to the third term in H_{SOC} equation [Fig. 2]. Furthermore, as a result of the second term in this equation, a tilting of the spin textures in the in-plane y direction is induced [Fig. 3]. It can therefore be concluded that the above spin-orbit Hamiltonian of the surface state matches well with the calculated results, i.e., the band split in the $\bar{\Gamma}$ - \bar{Y} direction and the tilt of the spin textures.

Since H_{SOC} is strongly affected by the electric field as mentioned above, the origin of the spin textures can be further clarified by studying the electric polarization.¹⁸⁾ On the basis that the spin-split surface state is strongly localized in the first two-bilayers [Fig. 4(a)], the strong electric polarization is expected to occur in these bilayers. To clarify this, the layer-dependence of the electric polarization was calculated using a point charge model (PCM) for Zn^{2+} and O^{2-} ions in the bilayer to evaluate the polarization difference: $\Delta \mathbf{P} = \mathbf{P}(c/a, u) - \mathbf{P}(c/a, u_{ideal})$. Here, c/a and u are the lattice constant ratio and internal parameter for a given optimized structure, respectively, and $u_{ideal} = 0.375$. As shown in Fig. 4(b), this reveals that the strongest electric polarization is identified near the first bilayer.

Electric polarization in the out-of-plane ΔP_z and in-plane ΔP_y directions was calculated to be 0.077 C/m² and -0.081 C/m², respectively. These values indicate that the electric field

in the out-of-plane E_z direction is comparable to that in the in-plane E_y direction, which would induce a tilting of the spin orientation [Fig. 4(c)]. However, only the in-plane electric polarization is observed in the case of bulk system [$\Delta P_{y\text{-bulk}} = -0.027 \text{ C/m}^2$]. This leads to the fact that the in-plane electric field E_y is generated, but induces a spin orientation with a fully out-of-plane z-direction [Fig. 4(d)].³⁵⁾ This would confirm that the spin textures in Fig. 3 are consistent with the PCM results.

Recently, PSH that induces a greatly enhanced spin relaxation time has been extensively studied,^{8–15)} with our calculations indicating that this is in fact achieved using the ZnO (10 $\bar{1}$ 0) surface. Since the spin textures in the calculated results show a quasi-one-dimensional orientation, a magnetic field is induced in a direction parallel to spin orientation. This inhibits the precession of the spins, thereby increasing the spin relaxation time. A similar mechanism behind long spin relaxation times has been reported in [110]-oriented zinc-blende QWs,^{36–38)} suggesting that the ZnO (10 $\bar{1}$ 0) surface could provide an efficient spintronics device.

The spin-orbit strength of the PSH (α_{PSH}), a variable of interest in spintronics device applications, was calculated using the band dispersion in Fig. 2. This found that the value of α_{PSH} is quite substantial (34.78 meVÅ) and much larger than what has been observed in the PSH of various zinc-blende n-type QW structures of GaAs/AlGaAs [(3.5 to 4.9 meVÅ),¹⁰⁾ (2.77 meVÅ)¹⁴⁾] and InAlAs/InGaAs [(1.0 meVÅ),¹²⁾ (2.0 meVÅ)¹³⁾]. This large value of α_{PSH} should ensure a small wavelength of PSH (λ_{PSH}), which is important to the miniaturization of spintronics devices. As it happens, the calculated value λ_{PSH} (0.19 μm) was in fact one-order less than that observed in the direct mapping of PSH (7.3 to 10 μm)¹⁰⁾ and the resonant inelastic light-scattering measurement (5.5 μm)¹⁴⁾ of GaAs/AlGaAs QWs.

In summary, by studying PSH on a ZnO (10 $\bar{1}$ 0) surface through first-principles DFT calculations, it has been shown that the spin textures exhibit a quasi-one-dimensional orientation. It was also found that the wavelength of this PSH is smaller than that observed on various zinc-blende quantum well structures. These results indicate that PSH can be achieved using a wurtzite (10 $\bar{1}$ 0) surface or interface with in-plane electric polarization and mirror symmetry, making it a suitable system for spintronics applications.

Acknowledgement

Part of this research was funded by the MEXT HPCI Strategic Program. This work was partly supported by Grants-in-Aid for Scientific Research (Nos. 25390008, 25790007, 25104714, 26108708, and 15H01015) from the Japan Society for the Promotion of Science (JSPS). The computations in this research were performed using the supercomputers at the Institute for Solid State Physics (ISSP) at the University of Tokyo. One of the authors (M.A.U.A) thanks to the Directorate General of Higher Education (DIKTI), Indonesia and Kanazawa University, Japan, for financial support through the Joint Scholarship Program.

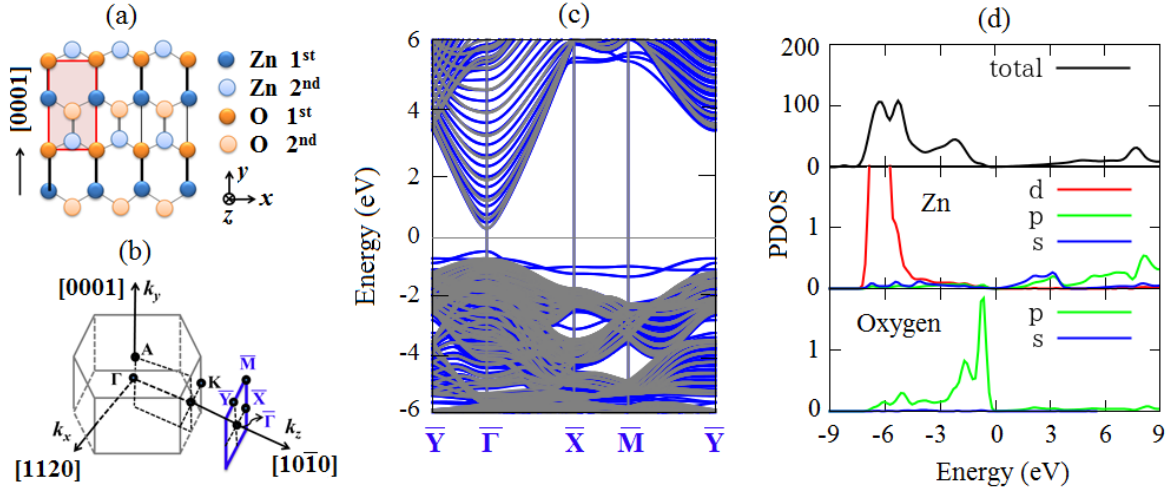


Fig. 1. (a) Top view of geometric structure of ZnO (10 $\bar{1}$ 0) surface. The polar direction [0001] is set to be the y direction. The unit cell of slab is indicated by the red line. (b) Schematic view of the first Brillouin zone of the crystal and the surface Brillouin zone. (c) Band structures of the surface. The blue lines correspond to the band structures of ZnO (10 $\bar{1}$ 0) surface and the black lines correspond to those of the bulk system. (d) Total density of states and partial density of states projected to the first-layer atoms.

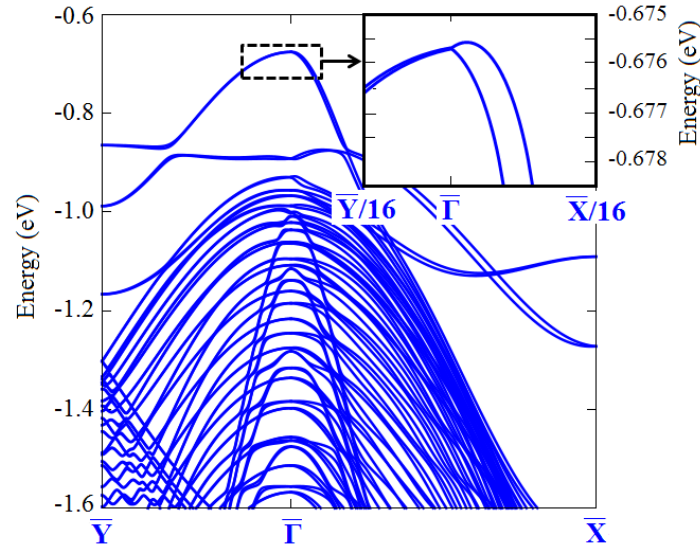


Fig. 2. Band structures near the VBM in the \bar{Y} - Γ - \bar{X} direction. The insert shows the spin-split surface-state bands.

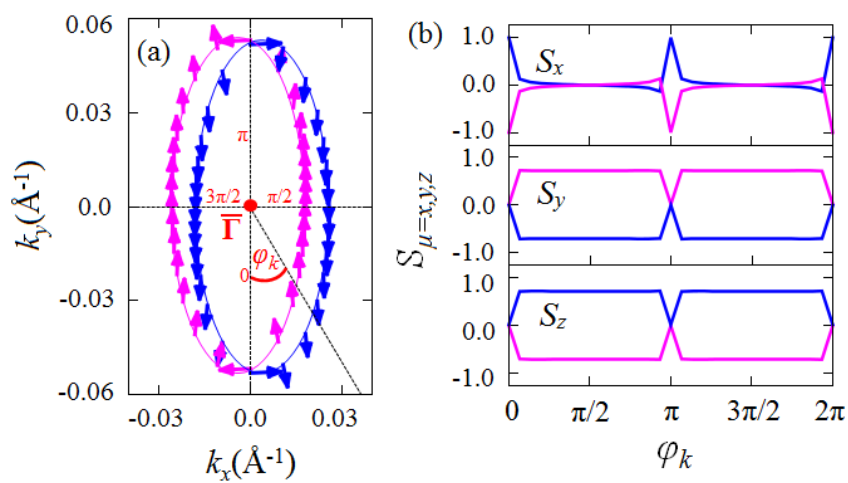


Fig. 3. (a) Spin textures of the surface states at the VBM. The band energy of the spin textures is 0.001 eV below the highest energy of the occupied surface state. The arrows represent the spin directions projected to the k_x - k_y plane. (b) Relationship between rotation angle (φ_k) and spin components is shown.

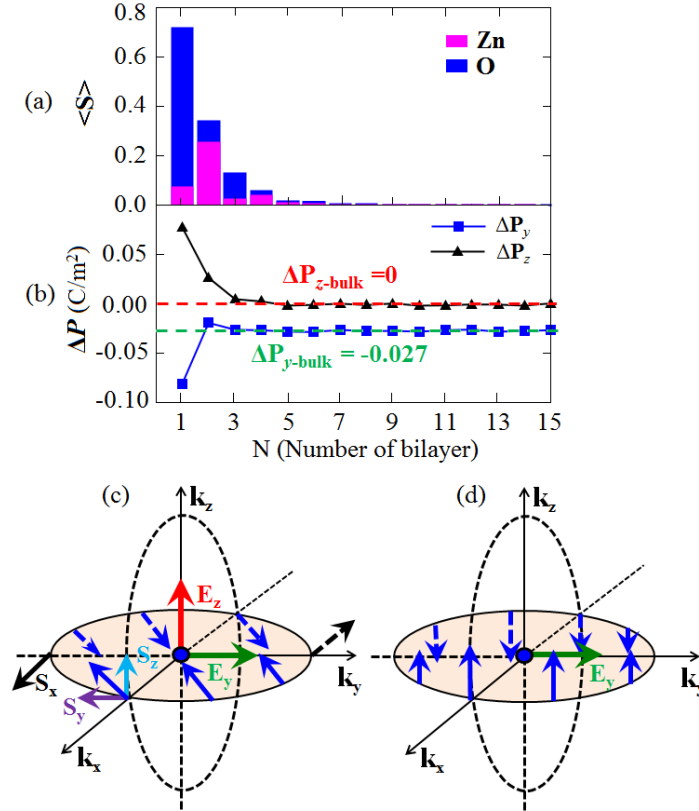


Fig. 4. (a) Expected values of spin projected to the atoms in each bilayers. The calculations are performed for the surface state in Fig. 3(a). The top of surface is represented by $N=1$. (b) Calculated data of the in-plane and out-of-plane electric polarizations (ΔP_y , ΔP_z) in each bilayers. The electric polarizations are calculated by using the PCM. Schematic view of the spin textures and electric fields for the case of the surface (c) and bulk systems (d).

References

- 1) Y. Kato, R. C. Myers, A. C. Gossard, and D. D. Awschalom, *Nature* 427, 50 (2004).
- 2) S. Kuhlen, K. Schmalbuch, M. Hagedorn, P. Schlamme, M. Patt, M. Lepsa, G. Guntherodt, and B. Beschoten, *Phys. Rev. Lett.* 109, 146603 (2012).
- 3) X.-L. Qi, Y.-S. Wu, and S.-C. Zhang, *Phys. Rev. B* 74, 085308 (2006).
- 4) J. Nitta, T. Akazaki, H. Takayanagi, and T. Enoki, *Phys. Rev. Lett.* 78, 1335 (1997).
- 5) S. Datta and B. Das, *Appl. Phys. Lett.* 56, 665 (1990).
- 6) T. Koga, J. Nitta, H. Takayanagi, and S. Datta, *Phys. Rev. Lett.* 88, 126601 (2002).
- 7) P. Foldi, B. Molnar, M. G. Benedict, and F. M. Peeters, *Phys. Rev. B* 71, 033309 (2005).
- 8) B. A. Bernevig, J. Orenstein, and S.-C. Zhang, *Phys. Rev. Lett.* 97, 236601 (2006).
- 9) J. D. Koralek, C. P. Weber, J. Orenstein, B. A. Bernevig, S.-C. Zhang, S. Mack, and D. D. Awschalom, *Nature* 458, 610 (2009).
- 10) M. P. Walser, C. Reichl, W. Wegscheider, and G. Salis, *Nat. Phys.* 8, 757 (2012).
- 11) M. Kohda, V. Lechner, Y. Kunihashi, T. Dollinger, P. Olbrich, C. Schonhuber, I. Caspers, V. V. Belkov, L. E. Golub, D. Weiss, K. Richter, J. Nitta, and S. D. Ganichev, *Phys. Rev. B* 86, 081306 (2012).
- 12) J. Ishihara, Y. Ohno, and H. Ohno, *Applied Physics Express* 7, 013001 (2014).
- 13) A. Sasaki, S. Nonaka, Y. Kunihashi, M. Kohda, T. Bauernfeind, T. Dollinger, K. Richter, and J. Nitta, *Nat. Nano.* 9, 703 (2014).
- 14) C. Schonhuber, M. P. Walser, G. Salis, C. Reichl, W. Wegscheider, T. Korn, and C. Schuller, *Phys. Rev. B* 89, 085406 (2014).
- 15) Y. S. Chen, S. Falt, W. Wegscheider, and G. Salis, *Phys. Rev. B* 90, 121304 (2014).
- 16) A. Tsukazaki, S. Akasaka, K. Nakahara, Y. Ohno, H. Ohno, D. Maryenko, A. Ohtomo, and M. Kawasaki, *Nat. Mater.* 9, 889 (2010).
- 17) O. Ambacher, J. Smart, J. R. Shealy, N. G. Weimann, K. Chu, M. Murphy, W. J. Schaff, L. F. Eastman, R. Dimitrov, L. Wittmer, M. Stutzmann, W. Rieger, and J. Hilsenbeck, *Journal of Applied Physics* 85 (1999).
- 18) M. A. U. Absor, H. Kotaka, F. Ishii, and M. Saito, *Applied Physics Express* 7, 053002 (2014).
- 19) J. P. Perdew, K. Burke, and M. Ernzerhof, *Phys. Rev. Lett.* 77, 3865 (1996).
- 20) T. Ozaki, H. Kino, J. Yu, M. J. Han, N. Kobayashi, M. Ohfuti, F. Ishii, T. Ohwaki, H. Weng, M. Toyoda, and K. Terakura: <http://www.openmx-square.org/>
- 21) N. Troullier and J. L. Martins, *Phys. Rev. B* 43, 1993 (1991).

- 22) T. Ozaki, Phys. Rev. B 67, 155108 (2003).
- 23) T. Ozaki and H. Kino, Phys. Rev. B 69, 195113 (2004).
- 24) H. Kotaka, F. Ishii, and M. Saito, Jpn. J. Appl. Phys. 52, 035204 (2013).
- 25) C. B. Duke, R. J. Meyer, A. Paton, and P. Mark, Phys. Rev. B 18, 4225 (1978).
- 26) B. Meyer and D. Marx, Phys. Rev. B 67, 035403 (2003).
- 27) P. Schroer, P. Kruger, and J. Pollmann, Phys. Rev. B 49, 17092 (1994).
- 28) N. L. Marana, V. M. Longo, E. Longo, J. B. L. Martins, and J. R. Sambrano, J. Phys. Chem. A 112, 8958 (2008).
- 29) H. H. Zhang, X. H. Pan, Y. Li, Z. Z. Ye, B. Lu, W. Chen, J. Y. Huang, P. Ding, S. S. Chen, H. P. He, J. G. Lu, L. X. Chen, and C. L. Ye, Applied Physics Letters 104, 112106 (2014).
- 30) P. Ding, X. Pan, J. Huang, H. He, B. Lu, H. Zhang, and Z. Ye, J. Cryst. Growth 331, 15 (2011).
- 31) T. Oguchi and T. Shishidou, Journal of Physics: Condensed Matter 21, 092001 (2009).
- 32) E. Simon, A. Szilva, B. Ujfalussy, B. Lazarovits, G. Zarand, and L. Szunyogh, Phys. Rev. B 81, 235438 (2010).
- 33) S. Vajna, E. Simon, A. Szilva, K. Palotas, B. Ujfalussy, and L. Szunyogh, Phys. Rev. B 85, 075404 (2012).
- 34) R. Requist, P. M. Sheverdyeva, P. Moras, S. K. Mahatha, C. Carbone, and E. Tosatti, Phys. Rev. B 91, 045432 (2015).
- 35) See supplemental material at [url will be inserted by publisher] for calculation results of the bulk system oriented on the $[10\bar{1}0]$ direction.
- 36) S. Dohrmann, D. Hagele, J. Rudolph, M. Bichler, D. Schuh, and M. Oestreich, Phys. Rev. Lett. 93, 147405 (2004).
- 37) O. D. D. Couto, F. Iikawa, J. Rudolph, R. Hey, and P. V. Santos, Phys. Rev. Lett. 98, 036603 (2007).
- 38) Y. Ohno, R. Terauchi, T. Adachi, F. Matsukura, and H. Ohno, Phys. Rev. Lett. 83, 4196(1999).